Integrative Biology

PAPER

View Article Online
View Journal | View Issue

The EGFR demonstrates linear signal transmission†

Cite this: *Integr. Biol.*, 2014, 6, 736

Diego A. Oyarzún,[a] Jo L. Bramhall,[b] Fernando López-Caamal,[c] Frances M. Richards,[d] Duncan I. Jodrell[bd] and Ben-Fillippo Krippendorff‡*[bd]

Received 21st March 2014,
Accepted 1st June 2014

DOI: 10.1039/c4ib00062e

www.rsc.org/ibiology

Cells sense information encoded in extracellular ligand concentrations and process it using intracellular signalling cascades. Using mathematical modelling and high-throughput imaging of individual cells, we studied how a transient extracellular growth factor signal is sensed by the epidermal growth factor receptor system, processed by downstream signalling, and transmitted to the nucleus. We found that transient epidermal growth factor signals are linearly translated into an activated epidermal growth factor receptor integrated over time. This allows us to generate a simplified model of receptor signaling where the receptor acts as a perfect sensor of extracellular information, while the nonlinear input–output relationship of EGF-EGFR triggered signalling is a consequence of the downstream MAPK cascade alone.

Insight, innovation, integration

We derived an analytical formula from nonlinear models of receptor signalling that have been used to model the signalling of the epidermal growth factor receptor (EGFR). The formula predicted that the cumulative EGFR signalling is linearly dependent on the ligand concentration outside the cell. Quantitative imaging of HeLa cells suggests that the cumulative EGFR signalling indeed depends linearly on the EGF concentration. Our mathematical approach therefore allows a simplified view on complex networks of receptor dynamics and describes the EGFR as a linear sensor of extracellular information encoded in ligand concentrations.

1 Introduction

Growth factors control a number of cellular responses such as proliferation, differentiation, apoptosis and angiogenesis. Despite our comprehensive knowledge of some of the processes involved in growth factor sensing and signalling, we still lack a quantitative grasp of how they modulate the transmission of growth stimuli to the nucleus. One of the obstacles is the presence of regulatory feedback loops acting on both surface receptors and downstream signalling, which obscure the input–output relationship between the ligand stimulus and the transmitted signal.[1] Moreover, growth factor signalling is a transient phenomenon because cells bind, internalize, and degrade ligands from the extracellular space. This causes receptor activation to weaken over the course of experiments, and thus extensive time course data are required to fully dissect the roles of individual processes.

The number of surface receptors available for binding is determined by receptor-related processes such as turnover, internalization, recycling and degradation.[2] As a consequence, cell surface receptors such as the epidermal growth factor receptor (EGFR) are increasingly being regarded as important regulators of downstream signalling.[1,3] The number of EGFR molecules at the cell surface is regulated by a number of dynamical processes (Fig. 1A): newly produced receptors are translocated to the cell membrane, while receptors at the cell surface are constantly exchanged with intracellular endosomal compartments *via* clathrin-mediated endocytosis.[4] Further, internalized receptors can be recycled to the cell surface from early endosomes and late recycling compartments by fusing with the plasma membrane.[5] Endosomes that are not recycled eventually fuse with lysosomes which lead to proteolysis of the attached receptors and the bound ligands.[6] The level of free EGFRs at the surface is therefore determined by the relative contributions of the individual trafficking and degradation processes.

[a] *Department of Mathematics, Imperial College London, UK*
[b] *Department of Oncology, University of Cambridge, UK*
[c] *Hamilton Institute, National University of Ireland, Maynooth, Ireland*
[d] *Pharmacology & Drug Development Group, Cancer Research UK Cambridge Institute, UK*

† Electronic supplementary information (ESI) available. See DOI: 10.1039/c4ib00062e

‡ Present address: Roche Pharmaceutical Research and Early Development, Pharmaceutical Sciences, Roche Innovation Center Basel, Grenzacherstrasse 124, 4070 Basel, Switzerland. E-mail: ben-fillippo.krippendorff@roche.com; Tel: +41616889732.

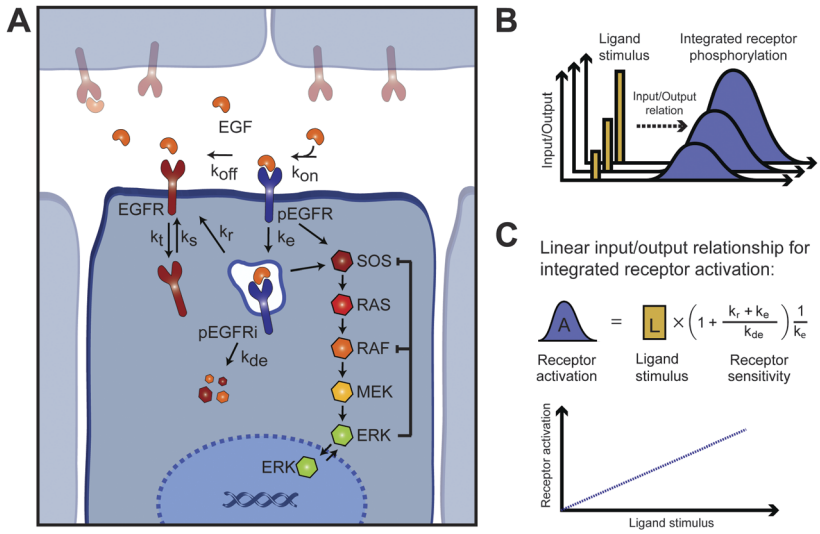

Fig. 1 Linear signal transmission in a model for epidermal growth factor receptor (EGFR) binding, turnover and trafficking. (A) EGF-induced signalling comprises ligand sensing by the EGFR on the cell surface, transmission of the sensed signal *via* the MAPK cascade, and nuclear import of active ERK. The extracellular EGF binds to free EGFR, triggering its dimerization and subsequent phosphorylation (pEGFR). Active receptors trigger the activation of the MAPK cascade and also get internalized by endosomes (pEGFRi). The endosomes are either degraded or recycled back to the cell surface. The MAPK cascade results in ppErk in the cytoplasm, which is finally imported into the nucleus to induce transcriptional changes. Eqn (1) is an ODE model of receptor binding, turnover and trafficking; the parameters are described in Table S1 in the ESI.† (B) Here we investigate the input–output relationship between a certain bolus extracellular stimulus (EGF concentration) and the resulting EGFR phosphorylation integrated over time (area under the activation curve). (C) The model predicts a linear input–output relationship between the ligand concentration and integrated receptor phosphorylation.

The ligands in the extracellular space also influence the fate of receptors at the cell membrane. Binding of ligands to the EGFR, for example, induces dimerization and autophosphorylation of intracellular residues.[7] These phosphorylations are responsible for the activation of different downstream signalling cascades, most prominently the mitogen-activated protein kinase (MAPK) cascade, composed of Ras-Raf-Mek-Erk, and the PI3K-Akt cascade.[8] At the same time, ligand binding perturbs the balance of the individual receptor trafficking processes by increasing the internalization rate of the EGFR.[9,10] *Via* this mechanism, receptor activation can potentially exert a negative feedback effect by increasing internalisation, and eventually degradation, of receptors and ligands in lysosomes.[1,11,12]

A number of mathematical models for the EGFR system have shed new light on the design principles underpinning growth factor signalling. One of the first examples was the steady state model of EGFR activation and trafficking by Wiley *et al.*[13] EGFR models have also proven useful to describe other receptor systems subject to the same processes (binding, internalization and recycling), but with parameter values that describe particular instances of a core network model.[14] Increasingly detailed models have been recently built to capture the mechanistic processes that control the input–output relationship of the EGFR system.[15]

Here we report our studies on the relationship between the extracellular ligand concentration and processes influencing EGFR signaling, such as ligand binding and receptor trafficking. We describe a previously unreported feature of EGFR signalling: its ability to linearly transmit extracellular ligand cues into cytoplasmic receptor activation. Using a combination of mathematical modelling, analysis and high-throughput imaging, we present evidence suggesting that receptor trafficking produces a linear input–output relationship between the initial ligand concentration and the cumulative receptor phosphorylation. The cytoplasmic signal in turn acts as an input to subsequent signalling cascades that cause signal saturation.

2 Materials and methods

Cell culture

The human cervical carcinoma HeLa cells were obtained from the CRUK Cambridge Institute and were authenticated by STR genotyping as well as tested negative for mycoplasma. These cells were maintained with Dulbecco's Modified Eagle Medium (DMEM) (Life Technologies Ltd, Paisley, UK) supplemented with 10% Fetal Calf Serum (FCS) (Life Technologies Ltd, Paisley, UK) at 37 °C in a humidified atmosphere of 5% CO_2 in atmospheric O_2 levels.

Immunofluorescence

Immunofluorescence was performed in ibidi 96-well plates (ibidi GmbH, Germany); cells were incubated at 37 °C for 24 h. After 24 h, the medium was replaced with medium containing no serum and incubated for a further 16 h at 37 °C. The cells were stimulated with 0, 6.25, 12.5, 25 and 50 ng ml^{-1} EGF (#01-101, Millipore, USA) at various time points, fixed with 4% paraformaldehyde in PBS and blocked with PBS/1% BSA (w/v)/0.1% saponin (w/v) (PBS/B/S) and 5% goat serum (v/v) (GS) for 1 h. The cells were incubated for 16 h at 4 °C with pEGFR (rabbit polyclonal anti-pEGFR Tyr1068, #3777 Ab, 1 : 600; Cell Signalling Technologies) and ppErk1/2 (mouse polyclonal anti-ppErk1/2

T185, Y187 T202 Y204, #ab50011 Ab, 1 : 500; Abcam). The plates were washed with PBS/B/S + 1% GS five times and incubated with secondary antibodies, antimouse IgG Alexa Fluor 488 (44085 Ab, 1 : 1000; Cell Signalling Technologies), antirabbit IgG Alexa Fluor 647 (44145 Ab, 1 : 1000; Cell Signalling Technologies) and DAPI (Invitrogen) for 1 h in the dark at room temperature. The plates were washed with PBS/B/S + 1% GS five times and stored in PBS at 4 °C in the dark until analysis.

High-throughput imaging

Quantitative imaging was performed by acquiring pictures of each well of the 96-well plate using the iCys Research Imaging Cytometer (CompuCyte, MA, USA) using 40× magnification and 405 nm, 488 nm, and 633 nm lasers. This microscope is purpose-built for the quantification of fluorescent signals in cells and is widely used for Laser Scanning Cytometry. Analysis of the field images is performed using the Columbus software (version 2.3, PerkinElmer) and Matlab (version 7.14, Mathworks). In each plate, two wells for each timepoint and treatment were measured. The data were then normalised in Prism (version 5, Graphpad) on each plate by defining the signal seen in the unstimulated wells as zero and the highest signal measured on the plate as one. Detailed information about the quantification of the field images and the data analysis pipeline can be found in Section S2 of the ESI.†

Mathematical modelling and analysis

The details of the mathematical methods can be found in the ESI.† Extensions of our method to compute the time-integrals of species concentrations in nonlinear reaction–diffusion models can be found in ref. 16.

3 Results

Exact computation of the integrated response in signalling networks

To investigate the relationship between EGFR trafficking and receptor activation, we first built an Ordinary Differential Equation (ODE) model for ligand binding, receptor trafficking, and turnover. The model comprises the receptor processes in Fig. 1A and describes the dynamic response of the ligand, free receptors, active receptors and endosomes:

$$\begin{aligned}\frac{\mathrm{d}L}{\mathrm{d}t} &= f(t) - k_{\mathrm{on}} R \cdot L + k_{\mathrm{off}} C + k_{\mathrm{r}} C_{\mathrm{int}},\\ \frac{\mathrm{d}R}{\mathrm{d}t} &= k_{\mathrm{s}} - k_{\mathrm{t}} R - k_{\mathrm{on}} R \cdot L + k_{\mathrm{off}} C + k_{\mathrm{r}} C_{\mathrm{int}},\\ \frac{\mathrm{d}C}{\mathrm{d}t} &= k_{\mathrm{on}} R \cdot L - k_{\mathrm{off}} C - k_{\mathrm{e}} C,\\ \frac{\mathrm{d}C_{\mathrm{int}}}{\mathrm{d}t} &= k_{\mathrm{e}} C - k_{\mathrm{r}} C_{\mathrm{int}} - k_{\mathrm{de}} C_{\mathrm{int}}.\end{aligned} \tag{1}$$

Here L is the concentration of the EGF ligand supplied to the medium at a rate $f(t)$, R is the concentration of free receptors (EGFR), C is the concentration of phosphorylated receptors (pEGFR), and C_{int} is the concentration of endosomes (pEGFRi). The parameters of the model are described in Table S1 in the ESI.† This model has been widely used to describe the EGFR and other receptor tyrosine kinase systems such as HER2,[14,16–19] as well as cytokine receptors such as the erythropoietin receptor (EpoR) and the interleukin-3 receptor.[14,20]

We focused on the relationship between the ligand concentration (dose) and the area under the receptor activation curve (see Fig. 1B). This time-integral represents the cumulative activation of the receptor over time and depends on the duration and peak of activation. The area under the activation curve is a good measure of a transient response and has proven useful to study signaling cascades,[21,22] reaction–diffusion systems,[23] cell surface receptors,[20] and was also found to link ERK activation with DNA synthesis.[24]

To study the input–output relationship of cellular signaling models, simulations are typically used to obtain sensitivities of outputs on the different model components. Conclusions drawn from simulation-based studies, however, can depend strongly on the specific parameter values used in the simulations. Moreover, model parameters are typically subject to high uncertainty due to the limited quantitative knowledge of the reaction kinetics and the limited datasets available for parameter estimation.

We here present an analytic approach to quantify the input–output relationship of cellular signaling models. To derive conclusions that are independent of the parameter values, we sought to analytically solve the time-integrals of the activated receptors as a function of the parameters. Signaling networks, however, display highly nonlinear dynamics and thus exact model solutions are hard (if not impossible) to obtain. We developed a mathematical approach to obtain exact formulae for the integrated response of signalling networks under external inputs.

We considered a signalling network with m reactions and n chemical species

$$\sum_{i=1}^{n} \alpha_{ij} s_i \xleftrightarrow{v_j} \sum_{i=1}^{n} \beta_{ij} s_i, \quad j = 1, 2, \ldots, m,$$

for $j = 1, 2, \ldots, m$. The variables s_i represent species concentrations, whereas α_{ij} and β_{ij} are the stoichiometric coefficients of species s_i in reaction v_j. To account for the interaction between the network and its environment, the species may be supplied to or consumed from the network at rate u_i. An ODE model for the network reads

$$\frac{\mathrm{d}s}{\mathrm{d}t} = Nv(s) + Du,$$

where s is the vector of species concentrations, v is the vector of reaction rates, and u is the vector of external stimuli. The stoichiometric matrix N has entries $N_{ij} = \beta_{ij} - \alpha_{ij}$; species s_i is consumed or produced in reaction v_j whenever $N_{ij} < 0$ or $N_{ij} > 0$. We modelled the effect of the stimuli with the matrix D, which determines which species are affected by the stimulus u_j (for example, to model an influx u_j of species s_i, we choose the jth column of D to have 1 in its ith entry and zeros elsewhere). We consider stimuli signals of the form $u(t) = \bar{u} + \delta(t)$, with $\bar{u}$ being a constant stimulus and $\delta(t)$ being a transient signal that vanishes to zero after sufficiently long time. After the transient stimuli have vanished, we assume that the network reaches a

unique and globally stable steady state $\bar{s}$ that matches the pre-stimulus steady state concentrations.

We obtained conditions on the network structure and reaction kinetics under which the integrated response of some of the species can be exactly computed from the formula:

$$\int_0^\infty (s_i - \bar{s}_i)\mathrm{d}t = f(p)(\tilde{s}_0 + u_T), \qquad (2)$$

where $\bar{s}_i$ is the steady state concentration of s_i, $f(p)$ is a nonlinear function of the model parameters (including for example, the stoichiometry and kinetic parameters), $\tilde{s}_0 = s_i(0) - \bar{s}_i$ is the initial deviation of s_i from its steady state concentration, and $u_T = \int_0^\infty \delta\,\mathrm{d}t$ is the net concentration of species supplied to the network by the transient signal $\delta(t)$. The formula in eqn (2) holds under conditions that depend on the stoichiometry and nonlinear kinetics, and describes the integrated response of s_i in terms of the kinetic parameters, initial concentrations and external stimuli. The derivation of the network conditions can be found in Section S1.1 and S1.2 of the ESI;† further extensions and interpretations of these conditions for spatio-temporal models can be found in ref. 16.

The EGFR displays linear signal transmission

Using our approach in the model for EGFR binding, turnover and trafficking (Fig. 1A), we found a simple linear input–output formula for the integrated receptor activation A:

$$A = \frac{1}{k_e}\left(1 + \frac{k_e + k_r}{k_{de}}\right) L_{total}, \qquad (3)$$

where L_{total} is the total concentration of the ligand supplied to the extracellular medium. The linear relationship is illustrated in Fig. 1B and C and its derivation can be found in Section S1.3 in the ESI.† For the considered model, the formula in eqn (3) is an exact description of the cumulative concentration of membrane-bound and internalised active receptors (pEGFR and pEGFRi in Fig. 1A) following a ligand stimulus; given the model-specific parameter values, the formula can be used to quantitatively predict the magnitude of receptor activation. The expression in

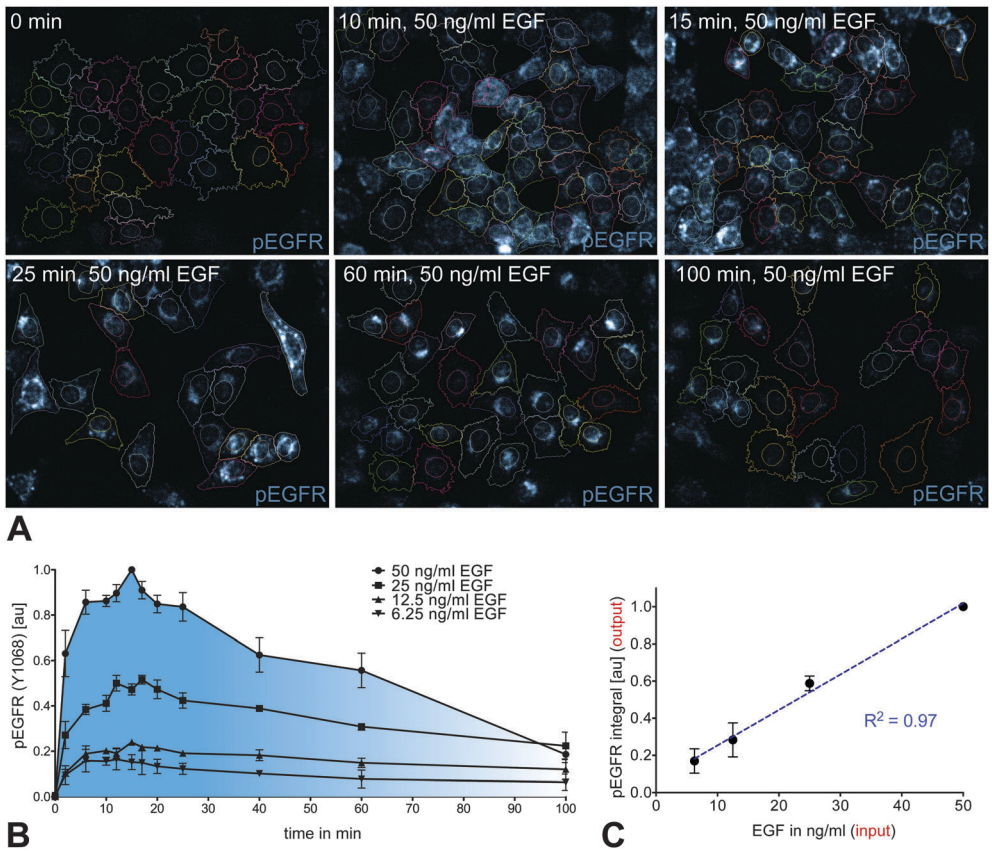

Fig. 2 Transient activation of the EGFR after stimulation of HeLa cells with different concentrations of EGF. (A) Serum starved HeLa cells were stimulated with 50 ng ml^{-1} EGF for different times; the chosen concentrations are within the range where EGFR phosphorylation was detectable *via* western blot, see ESI.† The cells were stained for DNA (DAPI) and pEGFR (Y1068) for imaging. Individual cells were identified based on DAPI staining and segmentation of the cytoplasmic staining as described in the Material and methods section. The EGF concentrations for stimulation were determined by western blotting (Fig. S4, ESI†). (B) Cytoplasmic and membrane staining was quantified for *ca.* 1500 individual cells per well. For each 96-well plate the data were normalised by dividing by the highest value per well observed over all timepoints. Data represent the mean of all quantified cells, while error bars represent the standard error between three biological replicates. (C) The measured pEGFR signal was integrated over time for the indicated concentrations of the EGF. Integrated activation was normalised to the highest value observed for the different ligand concentrations on the plate. Error bars represent the standard error between three biological replicates. The dashed line is a linear fit of the data.

(3) suggests that not all the processes affect the cumulative activation. In particular, receptor turnover (determined by k_t and k_s) as well as ligand binding (k_{on} and k_{off}) cancel out and do not affect the activation integrated over time. The formula for A therefore predicts that, despite the nonlinearities introduced by the limited amount of receptors available for binding, the integrated receptor activation scales linearly with the ligand concentration.

We then asked whether the predicted linearity is a consequence of the specific binding kinetics assumed in the model (described as a bimolecular mass action process), and consequently computed the integrated activation for a generic family of binding kinetics. We found that the linear signal transmission seems to be independent of the binding mechanism (see Section S1.4 in the ESI†) and furthermore, it should appear even when assuming saturable or cooperative binding.

Our result suggests that cumulative activation of EGFR depends on the trafficking processes, that is, on the interplay between receptor recycling, internalization and breakdown. Receptor trafficking therefore seems to be the key process enabling a broad dynamic range in EGFR signal transmission. Since this principle emerges independently of specific parameter values, it also suggests that it could be a robust property conserved across the family of receptors subject to trafficking, binding and turnover processes.

To experimentally test our theoretical prediction, we measured the temporal response of EGF-triggered phosphorylation of the EGFR in HeLa cells with high-throughput quantitative immunofluorescence imaging. We first determined the range of EGFR

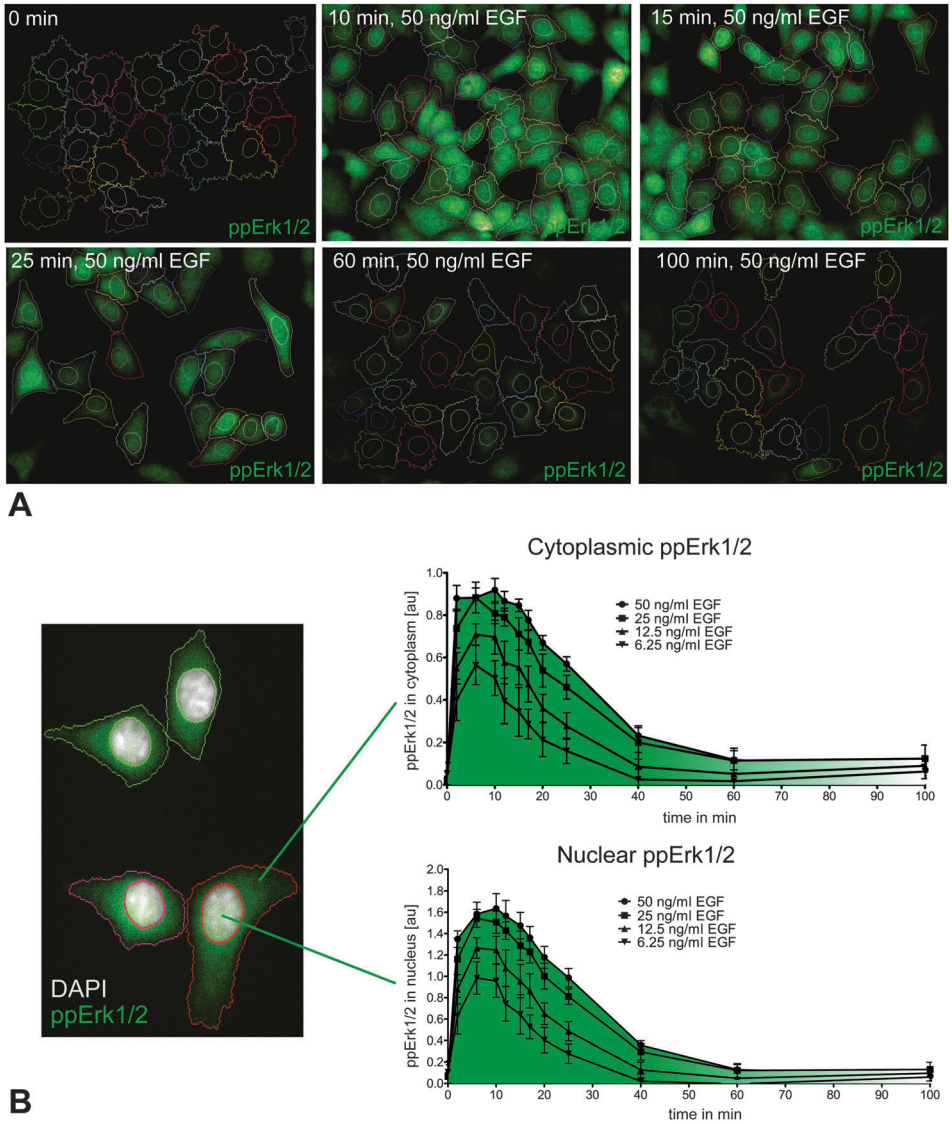

Fig. 3 Transient activation of ppErk1/2 after stimulation of HeLa cells with different concentrations of EGF. (A) In addition to EGFR quantification as shown in Fig. 2, ppErk1/2 (T185/Y187, T202/Y204) was quantified to investigate how the receptor signal is changed by downstream signalling. The measurements were obtained and normalized as described in Fig. 2. (B) To distinguish between cytoplasmic and nuclear levels of ppErk the nuclear area was contoured by DAPI staining as described in the Material and methods section. The nuclear ppErk signals were normalized by dividing by the highest value for the cytoplasmic area to allow for a comparison of cytoplasmic and nuclear values.

concentrations that resulted in measurable EGFR phosphorylation (details in the ESI†). For the batch of EGF used, EGFR phosphorylation was measured for concentrations above 10 ng ml^{-1} using quantitative western blotting. Next, we serum starved HeLa cells to eliminate all growth factor mediated EGFR phosphorylation and then stimulated the cells with 6.25 to 50 ng ml^{-1} EGF.

The imaging approach was used to determine the signal in different compartments of the cell. Further, single-cell imaging allows us to derive a mean value of thousands of individual measurements. We scanned 96-well plates using a laser cytometer and segmented individual cells from the collected images (Fig. 2A and details in Materials and methods). We then quantified in each cell the level of EGFR phosphorylation at Y1068, which is crucial for downstream signalling and activation of the MAPK cascade resulting in Erk1/2 activation.[9,25]

The mean EGFR phosphorylation peaked at around 15 min after EGF stimulation (Fig. 2B), followed by a slow reduction of the pEGFR signal corresponding to the internalization and degradation of the activated receptor after around 5–20 min.[26] At later timepoints localised intracellular staining close to the nucleus was apparent, most likely representing trafficking of the EGFR to the endoplasmic reticulum. We integrated the mean phosphorylation level of all measured cells over the timescale of the experiment (0–100 minutes). In agreement with our theoretical predictions, the integrated response of pEGFR was found to be proportional to the initial EGF concentrations (Fig. 2C), confirming that the EGFR linearly translates the extracellular EGF into an integrated response of receptor phosphorylation.

We suggest that the linear signal transmission may be a consequence of a negative feedback exerted by receptor trafficking. Processes such as receptor endocytosis, recycling and degradation processes determine receptor activation integrated over time and hence limit receptor signaling. As a consequence, the model suggests that in cancer cells mutations that reduce receptor internalization and degradation could be especially beneficial to maximize stimulation from a limited supply of growth factors. This could be another aspect of the important role of mutations that modify receptor trafficking in cancer.[27–30]

The MAPK cascade limits the dynamic range of signal transmission

Next we investigated how the linear signal of activated EGFR is transmitted into the cytoplasm and nucleus. In addition to pEGFR, we measured activated Erk1/2 in the cytoplasm and the nucleus (Fig. 3A) using an additional antibody specific to double phosphorylated Erk1/2. The high-throughput imaging approach hence allowed us to determine pEGFR and ppERK1/2 levels for individual cells.

We found that the time profile of Erk activation follows a similar shape to that of receptor activation, but reaches its peak earlier at around 8–10 min and drops sharper afterwards (Fig. 3B). This quick response of Erk1/2 upon upstream receptor activation has been previously ascribed to the ultrasensitive behaviour arising from double phosphorylation of ERK by MEK and positive feedback.[31–34]

However, in contrast to the linear response of the integrated pEGFR signal (Fig. 2C), it can be observed from the time profiles for 25 and 50 ng ml^{-1} the EGF triggers a nearly identical ppErk1/2 response (Fig. 3B). This means that the ppErk1/2 response saturates for high ligand concentrations, and hence suggests that the MAPK cascade may limit the dynamic range of signal transmission.

Using DAPI staining to contour the nuclear regions also allowed us to determine the localization of ppErk1/2 inside the cell (Fig. 3B). We found that the nuclear level of ppErk1/2 showed a similar time course as the cytoplasmic levels, but the staining intensity of ppErk1/2 was higher in the nucleus

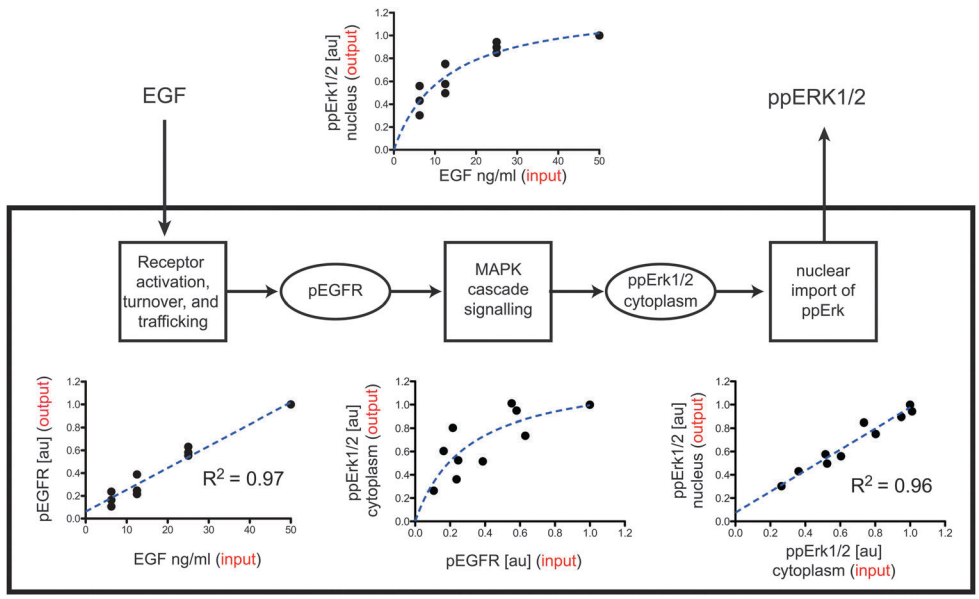

Fig. 4 Modular input–output description EGF signalling. The blocks represent subsystems and the arrows represent the signals interconnecting them. To determine the input–output relationship the integrals of the measured proteins are plotted against each other. Data points are individual biological replicates normalized to the highest value observed on one plate. Dashed lines are linear fits and the curves are Michaelis–Menten fits of the data.

than in the cytoplasm. This apparent amplification of the signal in the nucleus however could potentially be due to the bright field imaging, because cells are flattest at the cytoplasmic region and thus the cytoplasmic signal is integrated over a smaller volume than the nuclear signal.

Finally, to understand how each individual signalling stage contributes to signal transmission from the extracellular space to the nucleus, we integrated the ppErk1/2 response over time and deconvolved the EGF signalling data into three subsystems (Fig. 4) the receptor subsystem, the MAPK cascade, and the nuclear import of active Erk1/2. Both the receptor and nuclear import display linear signal transmission, whereas the MAPK cascade introduces a saturable response. The input–output relationship of the complete system therefore displays saturation, which limits the cellular sensitivity to stronger EGF stimuli. This suggests that the nonlinear relationship between the EGF concentration and cumulative nuclear ppErk1/2 results only from the dynamics of the MAPK cascade.

4 Conclusions

The link between growth factors and cellular responses depends on how extracellular signals are sensed and transmitted from the cell surface to the nucleus. In this article we used a modular approach to study how an EGF signal is transmitted by the EGFR system, the downstream MAPK signalling cascade, and the nuclear import of ppERK1/2. Our main finding is that the receptor system displays a linear input–output relationship between the ligand concentration and the cumulative receptor activation over time. We therefore conclude that the receptor system might act like a linear sensor, translating extracellular information proportionally into an intracellular signal.

Acknowledgements

DAO acknowledges the support from the Imperial College London Junior Research Fellowship Scheme. FLC acknowledges the support from the National Biophotonics and Imaging Platform, Ireland, funded by the Irish Government's Programme for Research in Third Level Institutions, Cycle 4, Ireland's EU Structural Funds Programmes 2007–2013. BFK, JLB, FMR and DIJ were funded by Cancer Research UK.

References

1 R. Avraham and Y. Yarden, *Nat. Rev. Mol. Cell Biol.*, 2011, **12**, 104–117.
2 I. Dikic and S. Giordano, *Curr. Opin. Cell Biol.*, 2003, **15**, 128–135.
3 G. Scita and P. P. Di Fiore, *Nature*, 2010, **463**, 464–473.
4 A. Sorkin and M. von Zastrow, *Nat. Rev. Mol. Cell Biol.*, 2002, **3**, 600–614.
5 H. Masui, L. Castro and J. Mendelsohn, *J. Cell Biol.*, 1993, **120**, 85–93.
6 K. Miller, J. Beardmore, H. Kanety, J. Schlessinger and C. R. Hopkins, *J. Cell Biol.*, 1986, **102**, 500–509.
7 A. M. Honegger, R. M. Kris, A. Ullrich and J. Schlessinger, *Proc. Natl. Acad. Sci. U. S. A.*, 1989, **86**, 925–929.
8 A. Citri and Y. Yarden, *Nat. Rev. Mol. Cell Biol.*, 2006, **7**, 505–516.
9 M. K. Nyati, M. A. Morgan, F. Y. Feng and T. S. Lawrence, *Nat. Rev. Cancer*, 2006, **6**, 876–885.
10 P. Gorden, J. L. Carpentier, S. Cohen and L. Orci, *Proc. Natl. Acad. Sci. U. S. A.*, 1978, **75**, 5025–5029.
11 H. T. McMahon and E. Boucrot, *Nat. Rev. Mol. Cell Biol.*, 2011, **12**, 517–533.
12 A. Sorkin and M. von Zastrow, *Nat. Rev. Mol. Cell Biol.*, 2009, **10**, 609–622.
13 H. S. Wiley and D. D. Cunningham, *Cell*, 1981, **25**, 433–440.
14 H. Shankaran, H. Resat and H. S. Wiley, *PLoS Comput. Biol.*, 2007, **3**, e101.
15 W. W. Chen, B. Schoeberl, P. J. Jasper, M. Niepel, U. B. Nielsen, D. A. Lauffenburger and P. K. Sorger, *Mol. Syst. Biol.*, 2009, **5**, 1–19.
16 D. A. Oyarzún, F. López-Caamal, M. R. García, R. H. Middleton and A. Y. Weiße, *PLoS One*, 2013, **8**, e62834.
17 K. A. Fujita, Y. Toyoshima, S. Uda, Y.-I. Ozaki, H. Kubota and S. Kuroda, *Sci. Signaling*, 2010, **3**, ra56.
18 P. Burke, K. Schooler and H. S. Wiley, *Mol. Biol. Cell*, 2001, **12**, 1897–1910.
19 H. Shankaran, H. S. Wiley and H. Resat, *BMC Syst. Biol.*, 2007, **1**, 48.
20 H. Resat, J. A. Ewald, D. A. Dixon and H. S. Wiley, *Biophys. J.*, 2003, **85**, 730–743.
21 V. Becker, M. Schilling, J. Bachmann, U. Baumann, A. Raue, T. Maiwald, J. Timmer and U. Klingmuller, *Science*, 2010, **328**, 1404–1408.
22 J. J. Hornberg, B. Binder, F. J. Bruggeman, B. Schoeberl, R. Heinrich and H. V. Westerhoff, *Oncogene*, 2005, **24**, 5533–5542.
23 R. Heinrich, B. G. Neel and T. A. Rapoport, *Mol. Cell*, 2002, **9**, 957–970.
24 A. R. Asthagiri, C. A. Reinhart, A. F. Horwitz and D. A. Lauffenburger, *J. Cell Sci.*, 2000, **113**(Pt 24), 4499–4510.
25 M. Rojas, S. Yao and Y. Z. Lin, *J. Biol. Chem.*, 1996, **271**, 27456–27461.
26 H. S. Wiley, S. Y. Shvartsman and D. A. Lauffenburger, *Trends Cell Biol.*, 2003, **13**, 43–50.
27 K. Roepstorff, L. Grøvdal, M. Grandal, M. Lerdrup and B. van Deurs, *Histochem. Cell Biol.*, 2008, **129**, 563–578.
28 A. Kirisits, D. Pils and M. Krainer, *Int. J. Biochem. Cell Biol.*, 2007, **39**, 2173–2182.
29 C. C. Reddy, A. Wells and D. A. Lauffenburger, *Biotechnol. Prog.*, 1994, **10**, 377–384.
30 Y. Mosesson, G. B. Mills and Y. Yarden, *Nat. Rev. Cancer*, 2008, **8**, 835.
31 A. Goldbeter and D. E. Koshland, *J. Biol. Chem.*, 1984, **259**, 14441–14447.
32 C. Y. Huang and J. E. Ferrell, *Proc. Natl. Acad. Sci. U. S. A.*, 1996, **93**, 10078–10083.
33 G. C. Brown, J. B. Hoek and B. N. Kholodenko, *Trends Biochem. Sci.*, 1997, **22**, 288.
34 J. E. Ferrell and E. M. Machleder, *Science*, 1998, **280**, 895–898.

